Draft version August 25, 2010
Preprint typeset using LaTeX style emulateapj v. 11/10/09

EVOLUTION OF GALAXY STELLAR MASS FUNCTIONS, MASS DENSITIES, AND MASS TO LIGHT RATIOS FROM $Z \sim 7$ TO $Z \sim 4$

Valentino González[1], Ivo Labbé[2,3], Rychard J. Bouwens[1], Garth Illingworth[1], Marijn Franx[4], Mariska Kriek[5]

Draft version August 25, 2010

ABSTRACT

We derive stellar masses from SED fitting for ~ 400 Lyman Break Galaxies at $z \sim 4$, 5, 6, and 7 from Hubble-WFC3/IR and Spitzer IRAC observations of the ERS field. Stellar Mass Functions (MFs) are determined from our new stellar mass M – UV luminosity relation and recent, deep UV Luminosity Functions (LFs). For the 299 $z \sim 4$ galaxies we find that the M–L_{UV} relation is a log-linear relation with a slope of $-1.7 \pm (0.2)$, which results in luminosity-dependent M/L_{UV} ratios, and large intrinsic scatter of ~ 0.5 dex. There is no evidence of M/L evolution from $z \sim 7$ to $z \sim 4$, suggesting that the specific SFR at a given mass does not evolve rapidly. Combining the observed M–L_{UV} relation with the UV LFs results in steep MFs with slopes $\alpha_M \sim -1.4$ to -1.6 at low masses. This slope, however, is flatter than the MFs obtained from recent hydrodynamical simulations. We use these MFs to estimate the Stellar Mass Density (SMD) to a fixed $M_{UV,AB} < -18$ as a function of redshift and find a SMD growth $\propto (1+z)^{-3.4\pm0.8}$ from $z \sim 7$ to $z \sim 4$. We also compare the SMD growth to that from the observed SFR density, accounting for the LF evolution by using an evolving limit of $0.2L^*(z)$. The resulting SMD growth $\propto (1+z)^{-2.8\pm0.9}$ shows a similar increasing trend to the integral of the SFR density $\propto (1+z)^{-6.3\pm0.6}$, but significant differences remain. These could result from too large dust corrections to the SFR at later times, stellar masses being overestimated at early times, or from non-monotonic star formation histories.

Subject headings: galaxies: evolution — galaxies: high-redshift

1. INTRODUCTION

One of the central questions in the study of high redshift ($z \gtrsim 4$) galaxies is the nature and timescale of their build-up and evolution. A key observable property for tracking this build-up is the stellar mass, which can be estimated from their rest-frame optical light as traced by Spitzer IRAC at $z > 4$. Measurements of the stellar mass provide us with important constraints on the previous star formation activity, particularly at times that we cannot access directly, thus helping reconstruct the star formation histories (SFHs) of high-redshift galaxies. For example, the evidence for a strong correlation between the current star formation rate (SFR) and stellar mass (Stark et al. 2009; Labbé et al. 2010a,b), with little apparent evolution between $z \sim 3$ and $z \sim 7$ (Stark et al. 2009; González et al. 2010), suggest that we are witnessing an epoch of exponential growth, similar to that found in simulations (e.g. Finlator et al. 2010).

The recent acquisition of deep near-IR WFC3/IR observations over the GOODS field allows us now to improve the stellar population modeling of star forming galaxies at $z \geq 4$ by expanding the SED fits into the UV. The improved data quality allows a better estimate of the rest-frame colors and mass-to-light (M/L) ratios.

Here we take advantage of the new WFC3/IR observations to do improved stellar population modeling on star-forming galaxies at $4 \leq z \leq 7$ within the ERS field (Windhorst et al. 2010). We revisit the relation between M/L_{UV} ratio and luminosity, characterize its scatter and use it in combination with the UV Luminosity Functions (LFs) to construct mass functions (MFs) at $z = 4$, 5, 6, and 7. We use these MFs to estimate the stellar mass density (SMD) of the universe at these redshifts and compare the observed growth with that expected from the integral of the SFR density.

Throughout this paper we adopt an $\Omega_M = 0.3$, $\Omega_\Lambda = 0.7$, cosmology with $H_0 = 70$ kms s^{-1} Mpc^{-1}. All magnitudes are in the AB system (Oke & Gunn 1983).

2. DATA AND SAMPLE

The sources presented here were found in the recently acquired Hubble-WFC3/IR observations over the Early Release Science (ERS) field (Windhorst et al. 2010) located in the northern section of the GOODS South field. Both the GOODS ACS optical (B_{434}, V_{606}, i_{775}, and z_{850} bands) and the WFC3/IR (Y_{098}, J_{110}, and H_{160} bands) data over this field reach depths of ~ 28 mag (5σ, $0.35''$-diameter apertures, see Bouwens et al. (2010); Giavalisco et al. (2004)). The GOODS program observations of this field with Spitzer/IRAC reach depths of 27.8 and 27.1 in the [3.6] and [4.5] channels respectively (1σ in $2.4''$apertures).

The sample is composed of 524 B, 123 V, and 32 i-dropouts. The criteria to select dropouts are the same as those used by Bouwens et al. (2007):

$z \sim 4$ B-dropouts:

$$(B_{435} - V_{606} > 1.1) \wedge [B_{435} - V_{606} > (V_{606} - z_{850}) + 1.1]$$

[1] Astronomy Department, University of California, Santa Cruz, CA 95064
[2] Carnegie Observatories, 813 Santa Barbara Street, Pasadena, CA 91101
[3] Hubble Fellow
[4] Leiden Observatory, Leiden University , NL-2300 RA Leiden, Netherlands
[5] Department of Astrophysical Sciences, Princeton University, Princeton, NJ 08544

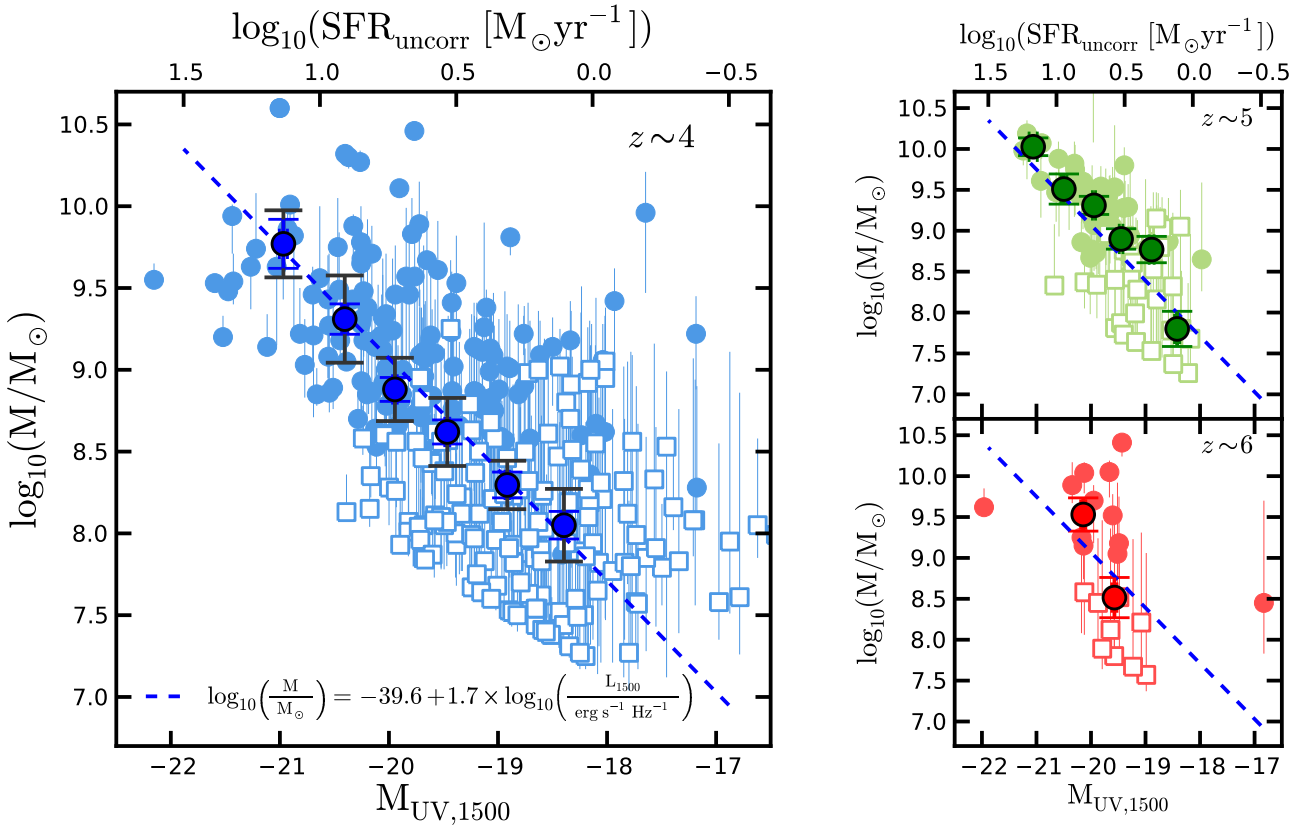

FIG. 1.— Stellar Masses from SED fits as a function of UV Luminosity ($M_{1500} = 51.63 - 2.5 \times \log_{10}(L_{1500}[\mathrm{erg\ s^{-1}\ Hz^{-1}}])$) for the $z \sim 4$,5, and 6 samples. SFR_{uncorr} is also shown and is derived using the Madau et al. (1998) conversion formula without correcting for extinction. The darker symbols in each panel represent the median log(M) of the sample in bins of ~ 0.5 $M_{1500,UV}$ mags. The small error bars represent the random error, while the larger ones give our estimate of the systematic error. The latter is computed by comparing the estimated median mass of galaxies at a given luminosity with the mass estimated from the stacked SEDs at the same luminosity. Open squares indicate sources that are undetected in the [3.6] IRAC channel ($< 2\sigma$). The dashed blue line represents the mean trend between $\log_{10}(M)$ and $\log_{10}(L_{UV})$ at $z \sim 4$. The best fit slope of $1.7(\pm 0.2)$, implies an increasing M/L ratio with luminosity. The scatter at the luminous end, where photometric errors are small, is intrinsic. No evidence is seen for evolution with redshift.

$$\wedge\ (V_{606} - z_{850} < 1.6)$$

$z \sim 5$ V-dropouts:

$$\{[V_{606} - i_{775} > 0.9(i_{775} - z_{850})]\ \vee\ (V_{606} - i_{775} > 2)\}$$
$$\wedge\ (V_{606} - i_{775} > 1.2)\ \wedge\ (i_{775} - z_{850} < 1.3)$$

$z \sim 6$ i-dropouts[6]:

$$(i_{775} - z_{850} > 1.3)\ \wedge\ (z_{850} - J_{125} < 0.8)$$

Due to the relatively broad PSF of IRAC, the images of our sources are usually contaminated by foreground neighbors. To obtain reliable IRAC fluxes we use the technique described in Labbé et al. (2006) to remove this contaminating flux (see also González et al. 2010; Labbé et al. 2010b,a; Wuyts et al. 2007; de Santis et al. 2007). In short, we use the higher resolution HST images to create models of each of the foreground neighbors and of the source itself. We convolve each of these model images with a kernel to simulate the IRAC observations modulo a normalization factor. We fit for all the sources simultaneously (each with an independent normalization factor) and subtract the best fit of all the neighbors. This way we obtain a clean image of the dropout and are able to perform standard aperture photometry. We use 2.4″-diameter apertures and correct the fluxes to total assuming stellar profiles (factor of 1.8 in both channels).

Our procedure for modeling and subtracting the light from nearby sources is not feasible for every dropout. By using the 70% of the sources with the best χ^2 residuals we reduce the non-optimal subtractions to $< 8\%$. This leaves 299, 78 and 24 of the original B, V and i-dropouts. We do not expect this criterion to introduce any important biases, since success depends mostly on how bright, complex, and close the non-associated neighbors are, and not on the source itself.

3. STELLAR POPULATION MODELING: STELLAR MASS ESTIMATES

We use the FAST SED fitting code (Kriek et al. 2009) to estimate redshifts, dust extinctions (A_V), ages, and the stellar masses of the $\sim$ 400 $z \sim 4$, 5, 6 and 7 sources based on broadband photometry. We use the (Bruzual & Charlot 2003, BC03) models with a Salpeter

[6] Slightly modified, Bouwens et al. 2010, in prep.

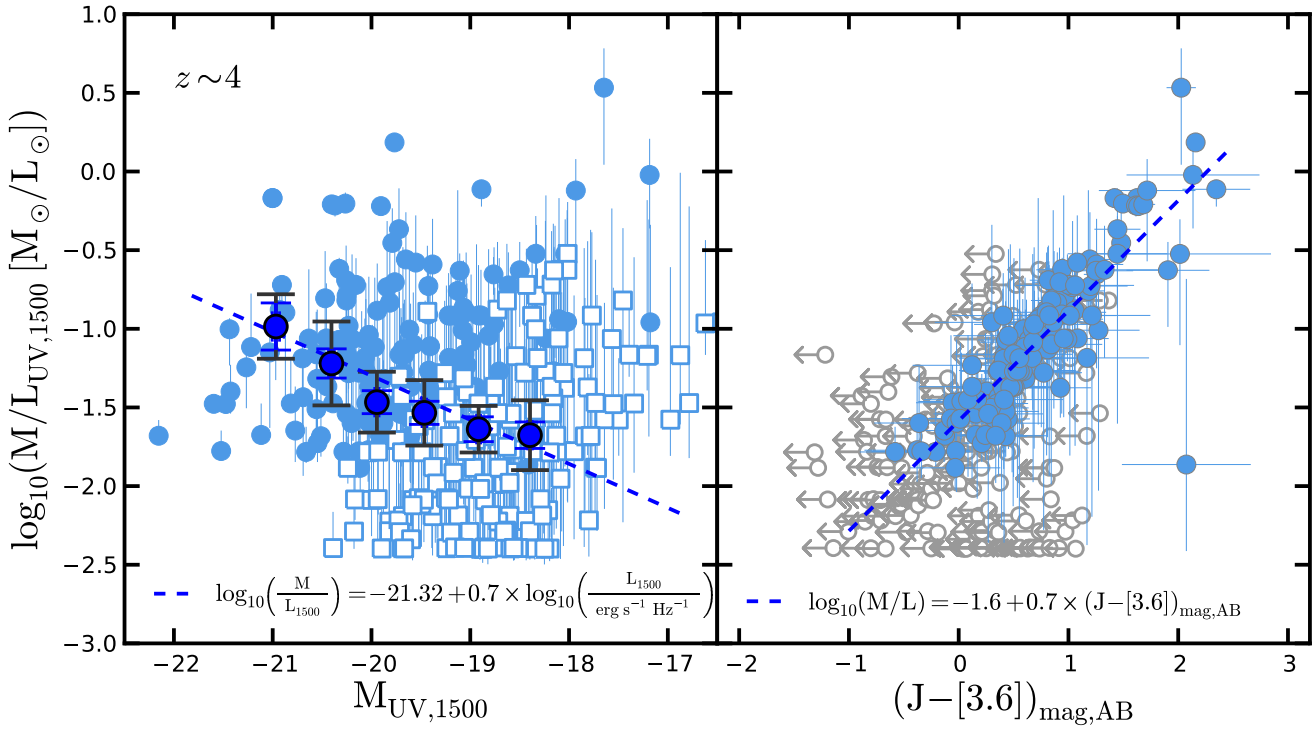

FIG. 2.— (*left*) M/L ratio as a function of UV Luminosity for the $z \sim 4$ sample. Symbols and error bars are as in Figure 1. The mean trend between stellar mass and UV Luminosity presented in Figure 1 (repeated here, dashed line) implies a M/L ratio that varies by ∼0.7 dex between the faintest and the brightest sources in our sample. (*right*) The tight correlation between M/L and $J-[3.6]$ color. Arrows indicate 2σ upper limits. This relation suggests that the large scatter observed in the M/L (left panel) is largely due to intrinsic variations in the UV-to-optical colors. Photometric scatter alone could only account for $\lesssim 0.14$ (0.37) dex at $\mathrm{M}_{1500} \sim -20$ (-19). This relation also allows us to estimate the effect that possible flux contamination to [3.6] by $H\alpha$ would have on the derived stellar masses (e.g., a 20% contamination would result in ∼ 30% overestimates of the masses).

(1955) initial mass function (IMF) from 0.1 to 100 $\mathrm{M}_\odot$. A Chabrier IMF would produce masses and SFRs ∼ 45% smaller (e.g. González et al. 2010).

The SFH cannot be uniquely determined from individual broadband SEDs due to well-known degeneracies between star formation timescale, age and dust extinction. We therefore assume a SFH with a constant SFR. Different SFHs primarily introduce systematic offsets to the mass determinations, largely independent of redshift (cf. Papovich et al. 2010). The systematic differences between masses based on declining, constant, or rising SFHs are typically $\lesssim 0.3$ dex (Finlator et al. 2007).

Figure 1 (left) shows the estimated stellar masses versus UV luminosity (bottom axis), and SFR (upper axis) uncorrected for dust extinction (using the Madau et al. (1998) relation). We find that the stellar mass M-L_{UV} relation at $z \sim 4$ is well approximated by a log-linear relation with a slope of 1.7(±0.2), with no significant evolution from $z = 6$ to $z = 4$.

Figure 2 explores the $z \sim 4$ M/L ratio trend in more detail, showing that $\mathrm{M/L}_{1500}$ depends on luminosity; the M/L is a factor ∼ 5 lower at $\mathrm{M}_{1500} = -18$ than at $\mathrm{M}_{1500} = -21$. This suggests that UV-faint galaxies contribute less to the global SMD than assumed in previous studies (Labbé et al. 2010b,a). However, due to the steep faint-end slope of the UV LF (e.g. Bouwens et al. 2010), their high density makes their total contribution significant.

A striking aspect of the relation is the large scatter in M/L. The observed scatter for our sample is ∼ 0.5 dex for $-21 < \mathrm{M}_{1500} < -18$. At the bright end $M_{1500} < -20$ the scatter is largely intrinsic, whereas at the faint end $M_{1500} > -19.5$ it is dominated by observational uncertainties. In particular, the stellar masses of sources with IRAC detections ($> 2\sigma$ in [3.6], 50% of sample) are much better constrained than IRAC undetected sources. Photometric uncertainties contribute ∼ 0.14 (0.37) dex to the scatter at $\mathrm{M}_{1500} \sim -20$ (-19). Moreover, we find that the M/L ratio is tightly correlated with the $J-[3.6]$ color (Figure 2, right), suggesting that the variation is real, and not an artifact of the modeling.

We can use the tight relation between color and M/L to estimate the impact of contamination by emission lines (not included in our models) on the derived stellar mass. For the B-dropouts, a 0.2 mag Hα contribution to the [3.6] flux implies a 0.14 dex lower M/L, or equivalently, lower SMDs by 30% at all redshifts.

4. MASS FUNCTIONS AND SMDS AT $Z \sim 4$, 5, 6, AND 7.

We derive the MFs at $z \sim 4$, 5, 6 and 7 using Monte-Carlo simulations. Starting with the UV LFs of Bouwens et al. (2007, 2010) at $z = 4$, 5, 6, and 7, we randomly select a set of Schechter parameters perturbed by the uncertainties and then draw 40000 values of M_{1500} following each distribution in the range $-21.5 < \mathrm{M}_{1500} < -18$. We convert M_{1500} to stellar mass

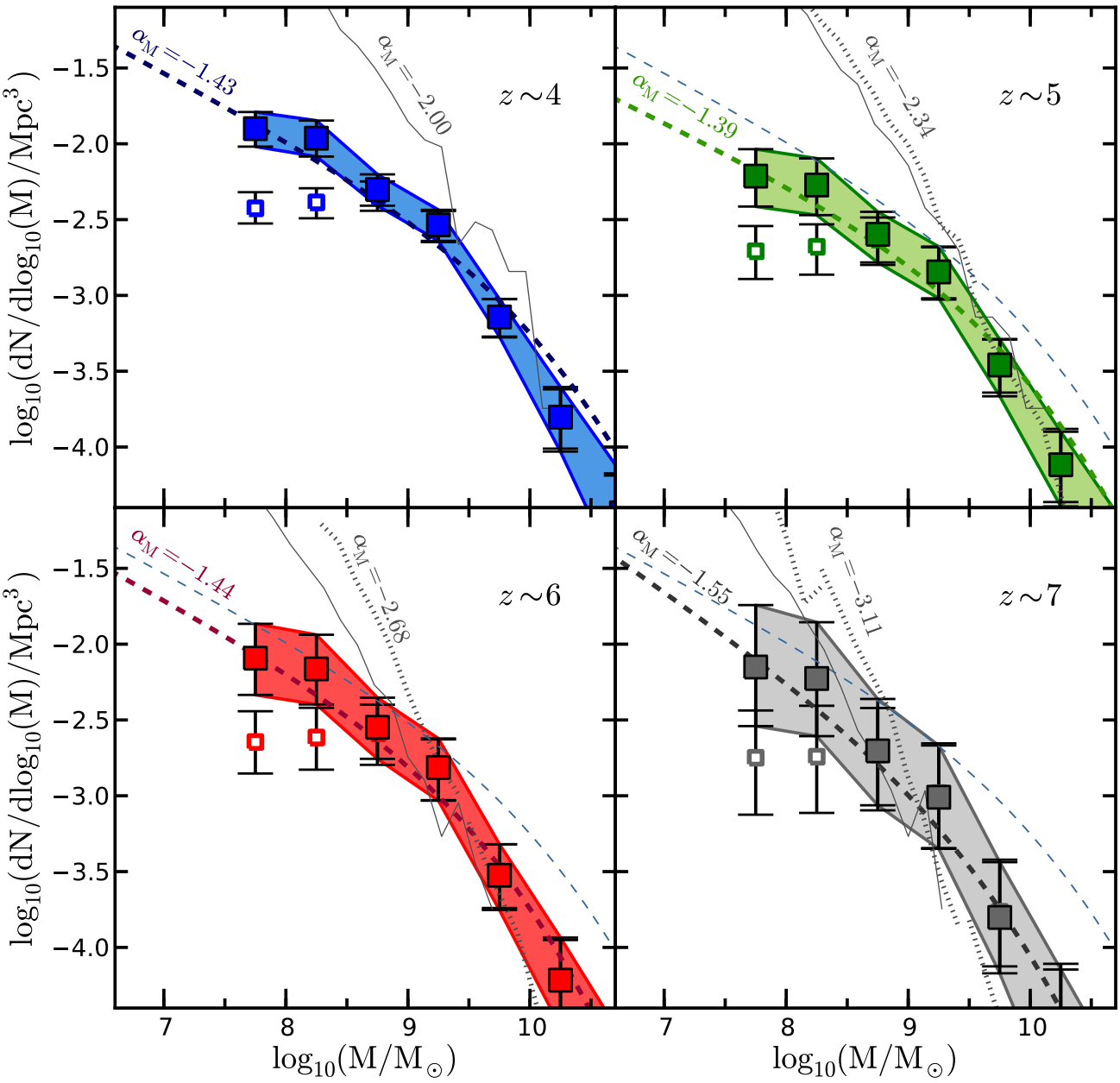

FIG. 3.— Stellar Mass functions at $z \sim 4$, 5, 6, and 7 derived from the stellar masses from SED fits, the $M - L_{UV}$ distribution for the $z \sim 4$ *B*-dropouts (Figure 1), and the UV LFs of Bouwens et al. (2007, 2010) at $z \sim 4$, 5, 6 and 7. Errors reflect uncertainties in both, the LF and the M-L relation. Open squares corresponds to MFs for sources brighter than $M_{1500} \sim -18$. Completeness corrections are estimated assuming that the M–L relation extends to fainter limits with similar scatter about the extrapolated mean trend (uncorrected: open; corrected: filled). The thick dashed curve in each panel represents the MFs obtained analytically based on the LFs, and an idealized log-linear $M - L_{UV}$ relation that extends to very faint limits with a log-normal spread of 0.5 dex. The $z \sim 4$ analytical MF is repeated in the other panels for comparison (thin dashed curve). The mass dependence of the M/L ratios results in analytic MFs with low mass slopes $\alpha_M \sim -1.4 - -1.6$, slightly flatter than the UV LFs ($\alpha = -1.7 - -2.0$, Bouwens et al. (2010)). In turn, the scatter of 0.5 dex enhances the number of sources at the high-mass end. The dotted / thin solid lines show the simulated MFs from Choi & Nagamine (2010) / Finlator et al. (in preparation). Their simulations produce many more low mass sources than we estimate here. This disagreement is quite unlikely to be caused by incompleteness at low masses.

by drawing random M/L ratios from the distribution at $z \sim 4$ with the same luminosity. We use the $z \sim 4$ distribution at higher redshifts because it is well-defined over a wide range of luminosities and the $z \sim 5$ and $z \sim 6$ distributions are consistent with that of $z \sim 4$. Since the Labbé et al. (2010a) relation at $z \sim 7$ is also consistent with the $z \sim 4$ relation, we have extended our calculation to that redshift. To correct the MFs for incompleteness at $M < 10^{8.5} M_{\odot}$, we re-derive the MFs but including fainter ($-18 < M_{1500} < -15$) sources, extrapolating the observed M–L relation to lower luminosities, and assuming that the low-luminosity scatter is similar to the scatter at $M_{1500} \sim -18.5$.

To better understand the shape of these MFs we model them analytically combining the UV LFs with a log-linear mass-luminosity relation that includes a log-normal scatter of 0.5 dex. The result is shown by the thick dashed curves in Figure 3. The scatter enhances the number of high-mass sources, producing excellent agreement with the observations. At lower masses, the slope of the MF is set by the faint-end slope of the UV LF and the M-L relation. Extrapolating this relation to lower luminosities results in steep low-mass slopes for the MFs of $-1.43(\pm0.11)$, $-1.39(\pm0.11)$, $-1.44(\pm0.15)$, and $-1.55(\pm0.21)$ at $z \sim 4$, 5, 6, and 7. These slopes are slightly flatter than the LF and considerably flatter than those obtained in recent hydrodynamical simulations (see Figure 3). Truncating the analytic M–L relation at $M_{1500} < -18$ results in flatter analytic MFs that are in close agreement with the non-corrected MFs.

We have integrated the directly determined MFs to $M_{1500} = -18$ to determine the SMD of the universe at $z = 4$, 5, 6, and 7 to faint luminosity limits (Table 1, Figure 4). Fitting the SEDs using the observed fluxes rather than upper limits allows us to reach lower limits than those of Stark et al. (2009) at $z = 4 - 6$. The integrated mass growth we derive with cosmic time is well fit by the function $\log_{10}(\mathrm{SMD}) \propto (1+\mathrm{z})^{-3.4\pm0.8}$.

5. STELLAR MASS GROWTH VS. STAR FORMATION RATE DENSITY

Comparing the stellar mass growth expected from the integral of the observed SFR density with the determination of the stellar mass growth as estimated from the MFs provides additional insights. Disagreement between these two approaches is expected if the SFH is especially bursty or if the IMF is variable or non-standard.

For self-consistency, we compare the stellar mass growth by following (approximately) the same population at all redshifts. We adopt an evolving lower limit that matches the evolution of the UV LF (e.g Reddy & Steidel 2009), since M^* brightens with cosmic time (e.g Bouwens et al. 2007, 2008, 2010). We take our luminosity limit to be the same as our $M_{1500} = -18$ search limit at $z \sim 7$ (Labbé et al. 2010a). This corresponds to $\sim 0.2L^*(z = 7)$. We evaluate our SMD estimates to the same limit of $0.2L^*$ at each redshift (Table 1 and Figure 4, right) and do the same for the SFR densities using the recent Bouwens et al. (2010) LFs. We integrate these SFR densities from $z \sim 100$ to $z \sim 4$ to derive the SMD (assuming $\mathrm{SFR}(z \sim 100) = 0$ and interpolating linearly). The integral of the SFRD includes mass loss due to stellar evolution using the BC03 models.

The SMD evolution versus the SFRD integral is shown in Figure 4 (right). Although the estimates trend similarly (within $\lesssim 0.3$ dex), the growth rate derived from SFRD $\propto (1+z)^{-6.3\pm0.6}$ appears markedly more rapid than the growth derived from SMDs $\propto (1+z)^{-2.8\pm0.8}$. If this difference is real, it could imply that the SFHs are less smooth than assumed here and galaxies are increasingly missed from dropout samples at later times (e.g., because of dust obscuration or passive evolution). Alternatively, the IMF could be variable or non-standard. Papovich et al. (2010) appear to find better agreement between the stellar mass and the SFR integral at $3 < z < 8$ for the brightest sources (selected at constant number density $n(< M'_{\mathrm{UV}}) = 2 \times 10^{-4}$ Mpc^{-3}) which may imply 100% duty cycles for the most luminous galaxies[7].

We caution, however, that our results only take into account random uncertainties, whereas systematics may affect both the derived stellar masses and SFRDs. For example, an overestimate of our dust corrections by a factor of ~ 2 at $z \sim 4$ would flatten the integrated SFRD to $(1+z)^{-4.9}$, whereas 0.2 dex lower masses at $z \sim 7-8$ would steepen the SMD growth to $(1+z)^{-3.6}$.

Another uncertainty is the difficulty of comparing the same population at early and late times. We assume here that the faintest galaxies evolve just like the typical L^* galaxy would, whereas Figure 1 suggests a faster evolution of the faintest sources if galaxies evolve along the M-L relation.

6. SUMMARY.

The availability of deep HST optical and near-IR, and Spitzer/IRAC observations over the ERS field provides us with an unprecedented opportunity to characterize the stellar populations of $z \gtrsim 4$ galaxies. By SED fitting the PSF-matched photometry we obtained for LBGs over this field, we have estimated stellar masses for ~ 400 $z \sim 4-7$ galaxies. We derive a relation between these masses and the observed UV luminosities at $z \sim 4$. We then combine this relationship with the UV LFs at $z \sim 4-7$ from Bouwens et al. (2007, 2010) to construct MFs and investigate the agreement between the inferred mass densities and those expected from the integral of the SFR density.

- We estimate a slope for the $\log_{10}(\mathrm{M}) - \log_{10}(\mathrm{L_{UV,1500}})$ relation of $\sim 1.7(\pm0.2)$ (Figure 1). This is steeper than the slope of 1.2 determined by Stark et al. (2009) at $z \sim 4$ and implies a luminosity-dependent M/L that decreases for fainter sources.

- We observe a sizable scatter of ~ 0.5 dex in the mass-luminosity relation at brighter luminosities ($M_{1500} < -20$) where the scatter can be robustly estimated. The tight correlation of M/L ratio with observed $J-[3.6]$ color suggests that the M/L scatter of bright sources is largely intrinsic (Figure 2).

- There is no evidence for strong evolution in the stellar mass - luminosity relation – and hence on the specific SFR – found from $z \sim 7$ to $z \sim 4$,

[7] In addition, the agreement in their Figure 3 may seem better as Papovich et al. (2010) derive a slightly shallower SFR(z) through a power law approximation and 0.2 dex lower masses at $z = 7-8$.

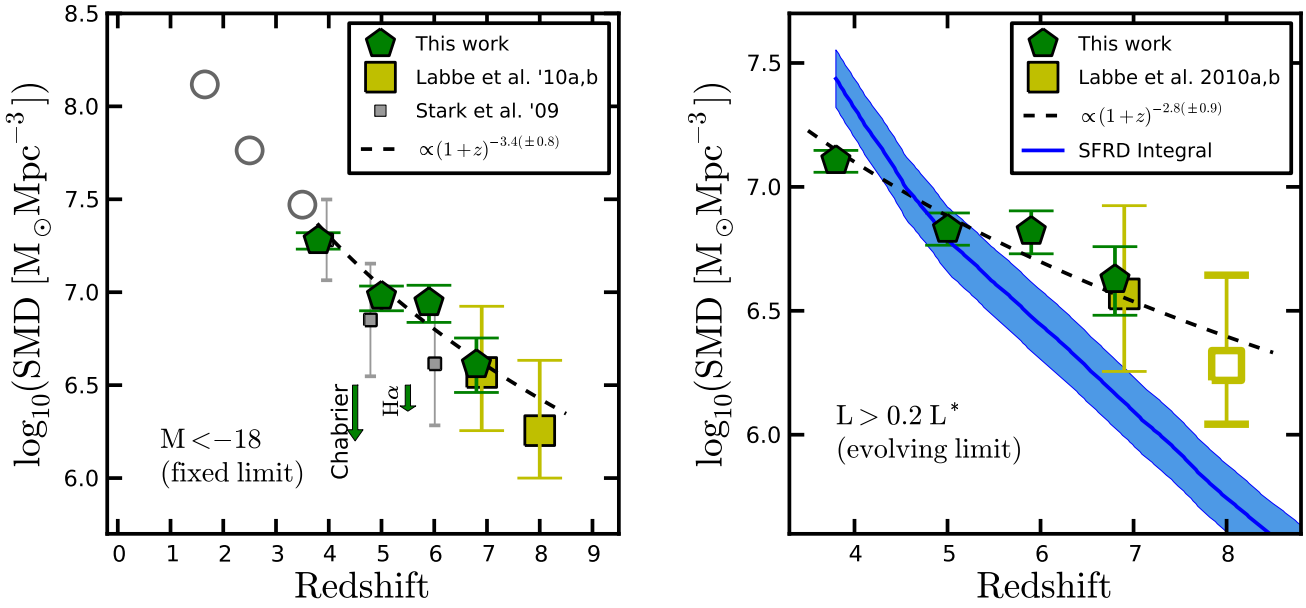

FIG. 4.— (*left*) Stellar Mass Density as a function of redshift for sources brighter than fixed $M_{1500,AB} = -18$. For comparison, we show the SMD determinations from Stark et al. (2009) corrected from their original $M_{1500} = -20$ limit to our $M_{1500} = -18$ limit by 0.18, 0.22 and 0.32 dex at $z \sim 4$, 5, and 6 respectively. The low redshift open circles were derived integrating the Marchesini et al. (2009) MFs between $8.3 < \log_{10}(M/M_\odot) < 13$ and multiplying by 1.6 to match the Salpeter IMF. A constant SFH and 0.2 $Z_\odot$ metallicity was assumed to derive the masses at $z \gtrsim 4$. (*right*) As for the left panel but varying the limit to a constant fraction of L^*. Comparison between the observed SMDs at high redshift and the values expected from the integral of the SFRD. We assumed that the SFHs of high redshift galaxies are smooth. To ensure that we are comparing the same population at each redshift, we correct the SMD and SFRDs for the evolution of the UV luminosity function, by integrating both to a relative limit of $0.2L^*_z$. This corresponds to imposing absolute limits of ~ 0.20, 0.15, 0.10, and 0.07 $L^*_{z=3}$ at $z \sim 4$, 5, 6, and 7 respectively. The SMDs that we derive from integrating the SFRD (assuming SFRD=0 at $z = 100$ and interpolating linearly) are broadly in agreement with what we infer from the MFs but with steeper growth. There are several possible explanations for the difference in the growth rate. One possibility is that the dust correction we utilize at $z < 5$ (from Bouwens et al. 2009) is too large – causing us to overproduce the SMD. A second possibility is that star formation in galaxies is non-monotonic and possibly subject to significant duty cycles – resulting in some incompleteness in UV-selected SMD probes at later times. A third possibility is that our modeling of the lower luminosity population may be inadequate (we assume it evolves in the same way as the luminous population). Stronger constraints require better mass estimates at $7 < z < 10$ and better dust content estimations at $z \sim 4$.

TABLE 1
SUMMARY OF RESULTS.

	$< z >= 3.8$	$< z >= 5.0$	$< z >= 5.9$	$< z >= 6.8$	$< z >= 8.0$
SMD (to $M_{1500} = -18$) $[10^6\ M_\odot]$	$18.96(^{+1.94}_{-1.90})$	$9.52(^{+1.27}_{-1.58})$	$8.79(^{+2.11}_{-1.91})$	$4.08(^{+1.59}_{-1.19})$	$1.8(^{+0.7}_{-1.0})$
Best Fit	$\log_{10}(\mathrm{SMD(z)}/[\mathrm{M}_\odot\ \mathrm{Mpc}^{-3}]) = 9.7(^{+0.6}_{-0.7}) - 3.4(^{+0.9}_{-0.75}) \times \log_{10}(1+\mathrm{z})$				
SMD (to $0.2L^*$) $[10^6\ M_\odot]$	$12.78(^{+1.26}_{-1.33})$	$6.74(^{+1.10}_{-0.93})$	$6.62(^{+1.39}_{-1.25})$	$4.23(^{+1.51}_{-1.19})$	···
Best Fit	$\log_{10}(\mathrm{SMD(z)}/[\mathrm{M}_\odot\ \mathrm{Mpc}^{-3}]) = 9.06(^{+0.7}_{-0.6}) - 2.8(^{+0.8}_{-0.9}) \times \log_{10}(1+\mathrm{z})$				
$\log_{10}$(SFRD) (to $0.2L^*$) $[\log_{10}(M_\odot\ \mathrm{yr}^{-1}\ \mathrm{Mpc}^{-3}]$	$-1.03(\pm0.11)$	$-1.67(\pm0.12)$	$-1.85(\pm0.14)$	$-2.01(\pm0.14)$	$-2.33(\pm0.14)$
SFR vs Stellar Mass (mean trend)					
$\log_{10}\left(\frac{\mathrm{SFR}}{[\mathrm{M}_\odot\ \mathrm{yr}^{-1}]}\right)$	$0.11(\pm0.06)$	$0.31(\pm0.06)$	$0.53(\pm0.07)$	$0.73(\pm0.06)$	$0.91(\pm0.06)$	$1.13(\pm0.05)$
$\log_{10}(M/M_\odot)$	$8.05(\pm0.60)$	$8.30(\pm0.59)$	$8.62(\pm0.53)$	$8.88(\pm0.54)$	$9.31(\pm0.50)$	$9.77(\pm0.50)$
Best Fit	$\log_{10}\left(\frac{\mathrm{M}}{\mathrm{M}_\odot}\right) = 7.8(\pm0.2) + 1.7(\pm0.2) \times \log_{10}\left(\frac{\mathrm{SFR}}{\mathrm{M}_\odot\mathrm{yr}^{-1}}\right)$				

[a] $M_{1500} = -18.13 - 2.5 \times \log_{10}(\mathrm{SFR_{uncorr}}[M_\odot\ \mathrm{yr}^{-1}])$

consistent with the findings of Stark et al. (2009); González et al. (2010); Labbé et al. (2010a,b).

- Using the steep UV LFs at $z \sim 4-7$ ($\alpha = -1.7 - -2.0$) and the mass-luminosity relation at $z \sim 4$ (both the mean relation and its scatter), we derive MFs in a self consistent way at $z \sim 4$, 5, 6, and 7 (Figure 3). We correct for incompleteness by assuming that the M-L relation extends to fainter magnitudes with similar scatter. The resulting MFs are quite steep. We derive analytical representations of these MFs and find low-mass slopes of $\sim -1.4 - -1.6$, which are significantly flatter than predicted by recent hydrodynamical simulations (Choi & Nagamine 2010). At the high-mass end of the MF, it is necessary to account for the scatter in M/L to match the enhanced number density.

- The SMDs derived from the MFs (to $M_{1500} < -18$) are well represented by the function SMD $\propto (1 + z)^{-3.4\pm0.8}$. This updates the relation presented in Labbé et al. (2010a).

- We compare the SMD estimated from the MFs at $z \sim 4-7$ with that expected from the integrated SFR density (Bouwens et al. 2010) using an evolving limit of $0.2L_z^*$ (where L^* brightens with cosmic time). Comparing the integral of the SFR density to the SMD (Figure 4, Table 1), we find that the observed growth rate is noticeably slower than that predicted by the SFR density ($(1+z)^{-6.3\pm0.6}$ vs $(1+z)^{-2.8\pm0.8}$). This could be caused by a possible overestimate of the dust extinction at $z \sim 4$, a modest duty cycle for the SF galaxies at $z \sim 4$, or shortcomings in our modeling of the faintest galaxies in our LBG search.

We acknowledge insightful discussions with Kristian Finlator, Casey Papovich, Daniel Schaerer, and Daniel Stark. We thank Ken Nagamine, Junhwnan Choi and Kristian Finlator for granting us access to their simulations. We also acknowledge support of grants HST-GO10937, HST-GO11563, and HST-GO11144. V.G. is grateful for the support from a Fulbright-CONICYT scholarship. I.L. is supported by NASA through a Hubble Fellowship grant #51232.01-A awarded by the Space Telescope Science Institute.

REFERENCES

Bouwens, R. J., et al. 2009, ApJ, 705, 936
Bouwens, R. J., Illingworth, G. D., Franx, M., & Ford, H. 2007, ApJ, 670, 928
—. 2008, ApJ, 686, 230
Bouwens, R. J., et al. 2010, ApJ, submitted, arXiv:1006.4360
Bruzual, G., & Charlot, S. 2003, MNRAS, 344, 1000
Choi, J., & Nagamine, K. 2010, MNRAS, 1042
de Santis, C., Grazian, A., Fontana, A., & Santini, P. 2007, New Astronomy, 12, 271
Finlator, K., Davé, R., & Oppenheimer, B. D. 2007, MNRAS, 376, 1861
Finlator, K., Oppenheimer, B. D., & Davé, R. 2010, ArXiv e-prints
Giavalisco, M., et al. 2004, ApJ, 600, L93
González, V., Labbé, I., Bouwens, R. J., Illingworth, G., Franx, M., Kriek, M., & Brammer, G. B. 2010, ApJ, 713, 115
Kriek, M., van Dokkum, P. G., Labbé, I., Franx, M., Illingworth, G. D., Marchesini, D., & Quadri, R. F. 2009, ApJ, 700, 221
Labbé, I., Bouwens, R., Illingworth, G. D., & Franx, M. 2006, ApJ, 649, L67
Labbé, I., et al. 2010a, ApJ, 716, L103
—. 2010b, ApJ, 708, L26
Madau, P., Pozzetti, L., & Dickinson, M. 1998, ApJ, 498, 106
Marchesini, D., van Dokkum, P. G., Förster Schreiber, N. M., Franx, M., Labbé, I., & Wuyts, S. 2009, ApJ, 701, 1765
Oke, J. B., & Gunn, J. E. 1983, ApJ, 266, 713
Papovich, C., Finkelstein, S. L., Ferguson, H. C., Lotz, J. M., & Giavalisco, M. 2010, arXiv:1007.4554
Reddy, N. A., & Steidel, C. C. 2009, ApJ, 692, 778
Salpeter, E. E. 1955, ApJ, 121, 161
Stark, D. P., Ellis, R. S., Bunker, A., Bundy, K., Targett, T., Benson, A., & Lacy, M. 2009, ApJ, 697, 1493
Windhorst, R. A., et al. 2010, arXiv:1005.2776
Wuyts, S., et al. 2007, ApJ, 655, 51